Bioorganic Chemistry 167 (2025) 109251

Contents lists available at ScienceDirect

Bioorganic Chemistry

journal homepage: www.elsevier.com/locate/bioorg

Targeting Tenascin-C-Toll-like Receptor 4 signalling with Adhiron-derived small molecules - a viable strategy for reducing fibrosis in systemic sclerosis

Thembaninkosi Gaule [a,1], Katie J. Simmons [b,1], Kieran Walker [c], Francesco Del Galdo [c], Rebecca L. Ross [c], Hema Viswambharan [b], Jahnavi Krishnappa [b], Jack Pacey [d], Martin McPhillie [d], Darren C. Tomlinson [e], Azhar Maqbool [b,*]

[a] Clinical Population and Sciences Department, Leeds Institute for Cardiovascular and Metabolic Medicine, School of Medicine, University of Leeds, Leeds, United Kingdom
[b] Discovery and Translational Science Department, Leeds Institute for Cardiovascular and Metabolic Medicine, School of Medicine, University of Leeds, Leeds, United Kingdom. School of Biomedical Sciences, Faculty of Biological Sciences & Astbury Centre, University of Leeds, Leeds, UK
[c] Leeds Institute of Rheumatic and Musculoskeletal Medicine, Faculty of Medicine and Health, University of Leeds, Leeds, United Kingdom; Scleroderma Programme, NIHR Leeds Musculoskeletal Biomedical Research Centre, Leeds, United Kingdom
[d] School of Chemistry, University of Leeds, Leeds, United Kingdom
[e] School of Molecular and Cellular Biology, University of Leeds, Leeds, United Kingdom

ARTICLE INFO

Keywords:
Tenascin C
TLR4
Adhiron
small molecules
fibrosis
systemic sclerosis

ABSTRACT

Tissue fibrosis is a hallmark of systemic sclerosis (SSc) and results from the persistent activation of fibroblasts and excessive accumulation of extracellular matrix component such as collagen. Recent evidence implicates the matricellular protein Tenascin-C (TNC) in promoting self-sustaining fibroblast activation and fibrosis *via* its interaction with Toll-like receptor 4 (TLR4). In this study, we utilized Adhiron-guided ligand discovery to identify small molecule inhibitors targeting the fibrinogen-like globe domain of TNC, a key mediator of TLR4 activation. Two lead compounds (464 and 830) demonstrated structural similarity, favourable ADME profiles, and robust anti-fibrotic activity *in vitro*. Treatment of dermal fibroblasts derived from SSc patients with either compound significantly reduced Transforming growth factor-β-induced expression of fibrotic genes, ACTA2, COL1A1, COL1A2, and CCN2, and inhibited myofibroblast differentiation. These studies may facilitate the development of effective targeted therapy for fibrosis in SSc and support this novel strategy for small molecule development.

1. Introduction

Persistent fibrosis a hallmark of systemic sclerosis (SSc) results from the excessive production and accumulation of collagen and other extracellular matrix (ECM) proteins by activated fibroblasts, leading to tissue disruption and dysfunction in the skin, lungs and other internal organs. Despite recent advances, clinical evidence reveals that up to one in three patients show fibrosis progression even while receiving

Abbreviations: ACTA2, Actin alpha 2 (alpha smooth muscle actin); cDNA, Complementary DNA; CIF, Cumulative incidence function; CLIA, Clinical laboratory improvement amendments; CMRI, Cardiac magnetic resonance imaging; COL1A1, Collagen type I alpha 1 chain; COL1A2, Collagen type I alpha 2 chain; CCN2, Cellular communication network factor 2 (connective tissue growth factor); DAMP, Damage associated molecular pattern; Dc-SSC, Diffuse cutaneous systemic sclerosis; ECL, Electrochemiluminescence; ECM, Extracellular matrix; EGF-L, Epidermal growth factor-like; EULAR ACR, European League Against Rheumatism/ American College of Rheumatology; FBG, Fibrinogen-like globe; FBG-C, Fibrinogen-like globe of tenascin C; FBS, Fetal bovine serum; FNIII, Fibronectin type III-like; FVC, Forced vital capacity; GAPDH, Glyceraldehyde 3-phosphate dehydrogenase; HRCT, High resolution computer tomography; HRP, Horse radish peroxidase; ILD, Interstitial lung disease; lcSSc, Limited systemic sclerosis; MAP, Multi-Anayte profiling; mRSS, Modified Rodnan skin score; PCR, Polymerase chain reaction; PFT, Pulmonary function test; Q-RT-PCR, Quantitative reverse transcription polymerase chain reaction; RHC, Right heart catherisation; ROCS, Rapid Overlay of Chemical Structures; RNA, Ribonucleic acid; SDS-PAGE, Sodium dodecyl-sulfate polyacrylamide gel electrophoresis; SSc, Systemic sclerosis; TGF-β, Transforming growth factor-β; TLR4, Toll-like receptor 4; TNC, Tenascin C; VEDOSS, Very early diagnosis of systemic sclerosis..

* Corresponding author.
E-mail address: cvsam@leeds.ac.uk (A. Maqbool).
[1] Joint 1st authors

https://doi.org/10.1016/j.bioorg.2025.109251
Received 22 May 2025; Received in revised form 28 October 2025; Accepted 12 November 2025
Available online 15 November 2025

recommended immunosuppressive or anti-fibrotic treatments [1–3] highlighting the urgent need for novel and more effective therapeutic strategies to treat SSc.

Recent studies have implicated a role for the matricellular protein and endogenous Damage Associated Molecular Pattern (DAMP), Tenascin C (TNC), in the pathogenesis of SSc. Tenascin C is highly upregulated in both the affected tissue and circulation of SSc patients with both early and late-stage disease. It is markedly expressed in skin and lung biopsies and in blister fluid in SSc patients, and elevated serum levels of TNC correlate with the Modified Rodnan skin score, a measure of skin fibrosis [4,5]. Dermal fibroblasts explanted from SSc patients show constitutive production of TNC *in vitro*, implying that its increased accumulation in SSc may result, in part, from its cell-autonomous overproduction [4]. Moreover, treatment of healthy fibroblasts with the profibrotic cytokine TGF-β, which is strongly implicated in the pathogenesis of SSc, induces the synthesis of TNC, whereas TNC deficiency attenuates TGF-β-mediated fibrosis *in vivo* following murine lung injury [6].

Tenascin C has been shown to elicit Toll like receptor 4 (TLR4)-dependent profibrotic responses in dermal fibroblast, including promoting myofibroblast differentiation, upregulation of αSMA and collagen expression [4]. In support of this, mice lacking TNC are protected from both skin and lung fibrosis following bleomycin injury [4,6,7]. Similarly, loss of either TNC or TLR4 is associated with reduced hypodermal fibrosis in the Tsk/+ mouse, a spontaneous fibrosis model [4,8]. Importantly, the profibrotic effects of TNC are completely abrogated in TLR4-deficient fibroblasts and by small molecules inhibitors that selectively block TLR4 underscoring a key pathogenic role for TNC-TLR4 signalling in driving persistent fibrosis [9,10].

These observations support a model of self-sustaining fibroblast activation in SSc, where tissue damage induces local TNC production that activates TLR4, promoting fibrotic gene expression and myofibroblast differentiation. This persistent fibroblast activation leads to continued matrix deposition, further tissue damage, and more TNC, so establishing a non-resolving loop of pathological fibrosis characteristic of SSc [9]. Targeting this loop is a promising therapeutic strategy for SSc-related fibrosis.

Tenascin-C is a multi-domain protein, with its fibrinogen-like globe (FBG) domain critical for TLR4 binding and activation [11–14]. Targeting this domain to prevent its interaction with TLR4 offers a promising anti-fibrotic approach. More so, as conventional TLR4 inhibitors have proven ineffective in clinical trials and may risk compromising the host response to infection [15], underscoring the need for selective strategies.

The Adhiron (formally known as Affimer) technology is a novel platform based on a highly diverse library ($>3 \times 10^{10}$) of small, engineered binding proteins, each displaying two variable nine-amino acid loops [16]. This platform enables high affinity, selective binding to specific target proteins. Adhirons have been successfully employed to identify functional regions, probe protein function and uncover druggable pockets on previously considered undruggable proteins such as Ras [17–26]. Analogous to antibodies [27], Adhirons can also serve as valuable tools for small molecule drug discovery with the potential act as pharmacophore templates that inform design and reduce the risk of failure in early development.

In the present study we have employed Adhiron guided ligand discovery to develop small molecules that target the FBG domain of TNC. Two of these compounds are shown to attenuate the profibrotic phenotype of human dermal fibroblasts following stimulation with Transforming growth factor-β (TGF-β), a key mediator of TNC expression and fibroblast activation [11].

2. Material and methods

2.1. Adhiron guided small molecule discovery

2.1.1. Production and purification of recombinant FBG protein

The genes encoding the FBG domains from human were synthesised by Genscript (Piscataway, USA). The FBG coding regions were amplified by PCR, digested with *Nhe*I and *Not*I, and cloned into a similarly digested pGEX vector modified to contain a N-terminal AviTag and C-terminal 8His tag. The FBG domains were expressed in Shuffle cells (NEB). Single colonies were used to inoculate 5 mL of LB media with 100 μg/mL disodium carbenicillin and grown at 37 °C with shaking at 220 rpm for 16 h. The overnight culture was used to inoculate large scale cultures of 400 mL pre-warmed LB medium with 100 μg/mL carbenicillin and grown at 37 °C, and 220 rpm. When OD600 reached 0.6–0.8 expression was induced using 0.1 mM IPTG and grown for a further 16 h at 25 °C with shaking at 150 rpm. Cells were harvested and resuspended in lysis buffer (50 mM NaH_2PO_4; 300 mM NaCl; 30 mM Imidazole; 10% Glycerol; pH 7.4) with 0.1 mg/mL of lysozyme, 1% Triton X-100, 10 U/ml Benzonase® endonuclease and 1× Halt protease inhibitor cocktail and incubated at 4 °C for 1 h. The FBG domain were purified from the supernatant using a two-step purification procedure, Ni^{2+}-NTA chromatography followed by size exclusion chromatography. The supernatants were filtered through a 0.2 μm syringe filter prior to loading on a homemade Ni^{2+}-NTA columns. The protein-bound columns were washed with wash buffer (50 mM NaH_2PO_4; 500 mM NaCl; 20 mM Imidazole; pH 7.4) to remove unbound proteins. 50 mM NaH_2PO_4, 500 mM NaCl; 300 mM Imidazole; pH 7.4 was used to elute bound FBG. The purity of the samples was assessed by SDS-PAGE with Coomassie staining and the elution fractions were pooled accordingly. The pooled samples were loaded onto a HiLoad® 26/600 Superdex® 200 size exclusion column, eluted in PBS and concentrated using Vivaspin® centrifugal concentrators with 10 kDa cut-off.

2.1.2. Phage display

Adhiron selection was performed as described previously [28,29] using a phage display library constructed by the BioScreening Technology Group (BSTG), University of Leeds, UK. Adhiron selection was performed as described previously [28]. Briefly, biotin acceptor peptide (BAP) human Tenascin-C FBG was bound to streptavidin-coated wells (Pierce) for 1 h. Following 3 h of pre-panning, the phage were incubated in wells containing human Tenascin-C FBG domain for an hour. Unbound or weak binding phage were washed away using PBST. Bound phage was eluted with 50 mM glycine–HCl (pH 2.2) for 10 min, neutralised with 1 M Tris–HCL (pH 9.1), further eluted with 100 mM triethylamine for 6 min, and neutralised with 1 M Tris–HCl (pH 7). After three biopanning rounds, 96 randomly picked positive Adhiron clones were evaluated for their binding ability to FBG by phage ELISA. Phage Elisa was undertaken in the manner we have previously described, briefly, recombinant FBG was immobilised directly on the plastic surface of 96-well Nunc MaxiSorp® plates (Thermo Scientific, Waltham, MA, US). The binding of Adhiron clones was detected with the use of 3,3′,5,5’-Tetramethylbenzidine. DNA was sent for DNA sequencing to allow analysis of the binding loop sequences.

2.1.3. Production of Adhiron protein and purification

Recombinant production of the Adhiron proteins was performed as previously described [28]. Briefly, the relevant Adhiron coding regions were amplified by PCR, using Forward primer (5′-ATGGCTAG-CAACTCCCTGGAAATCGAAG) and Reverse primer (5′- TACCC-TAGTGGTGATGATGGTGATGC). The products were digested with *Nhe*I and *Not*I restriction enzymes at 37 °C for 2 h and cloned into a similarly digested pET11a vector modified to contain an 8’His tag coding sequence. BL21 STARä (DE3) cells were transformed using the relevant cloned and cultured as described in Tiede et al. [28]. The cells were harvested and resuspended in phosphate buffered saline pH 7.4

supplemented with 0.1 mg/mL of lysozyme, 1% Triton X-100, 10 U/mL Benzonase® endonuclease and 1× Halt protease inhibitor cocktail and incubated at 4 °C for 1 h. Adhirons were purified from supernatant using Ni^{2+}-NTA affinity chromatography as previously described [28].

2.1.4. Solid phase inhibition assays

Streptavidin coated 96-well plates were blocked overnight at 4 °C using 2 × blocking buffer (Sigma) in PBS-T (0.1% Tween-20). 5 μg/mL of Bap tagged hFBG-C was immobilised onto the pre blocked streptavidin coated 96 well plates for 1 h at room temperature. Unbound Bap tagged hFBG-C was washed off using PBS-T. 25 μg/ml of Adhiron was then added to appropriate wells and incubated for 1 h at room temperature with gentle agitation. Excess Adhiron was removed by washing three times with PBST. To assess the Adhiron protein's ability to block the hFBG-C/TLR4 25 μg/mL of TLR4 was added to the wells and incubated for 2 h at room temperature. TLR4 binding was detected as described previously [30]. After three washes TLR4 binding was visualised by adding 50 μl of TMB and measuring absorbance at 620 nm. Experimental controls involved probing for TLR4 binding in the absence of Adhiron.

2.1.5. Crystallization, data collection, and structure determination

8His tagged human FBG binding Adhiron and untagged human FBG were expressed in BL21 DE3 star and shuffle cells respectively. The cells were harvested by centrifugation at 10000 *g* for 20 mins. The pellets resuspended in PBS supplemented with benzonase, Triton X-100, and lysozyme were incubated at room temperature with gentle agitation for 1 h. The 8His tagged Adhiron protein was immobilised onto Ni-NTA beads by incubating the Adhiron protein containing lysate with Ni-NTA agarose beads for 1 h at room temperature. Following the 1 h incubation the Ni-NTA beads were washed to remove unbound Adhiron protein. The Ni-NTA beads carrying Adhiron were then added to the human FBG containing lysate and incubated for 1 h at room temperature. The beads were washed and the Adhiron/human FBG complex was eluted using PBS supplemented with 300 mM imidazole. The contents of the elutions were analysed using SDS-PAGE and the appropriate elutions were pooled, concentrated, and further purified using and size exclusion column (HiLoad® 26/600 Superdex® 200). The Adhiron/human FBG complex was concentrated to 30 mg/ml and crystallised using the sitting drop method and the MCSG-3 crystal screen (molecular dimensions). The crystal belonged to space group P 21 21 21 with cell dimensions a = 77.570 Å,b = 90.140 Å and C = 104.410 Å and a = b = g = 90. The Adhiron/human FBG structure was determined using molecular replacement.

2.1.6. Ligand-based virtual screening

A shape similarity screen was performed using OpenEye's ROCS software [31]. ROCS allows rapid identification of active compounds by shape comparison, through aligning and scoring a small molecule database against a query structure of residues N41, H43 and D47 from Adhiron 52. The EON software compares electrostatic potential maps of pre-aligned molecules to a query structure, producing a Tanimoto similarity score for comparison. This was used in conjunction with the eMolecules library of 10,000,000 commercially available small molecules. Identification of compounds best matching the shape and electrostatic properties of the Adhiron residues interacting with FBG was carried out using the graphical user interface Maestro [32] and the OpenEye graphical user interface VIDA looking for specific hydrogen bonding interactions with FBG and minimising any steric clashes with the protein. This work was undertaken on ARC4, part of the High-Performance Computing facilities at the University of Leeds. Molecules were selected for biological evaluation based on favourable shape and electrostatic matching to the query residues.

2.1.7. Metabolic stability and solubility assessment

This was carried out by Eurofins Ltd. according to their standard protocols.

2.1.8. Surface plasmon resonance

A Biacore 1K (Cytiva, USA) was used to analyse the interaction between fibrinogen and a small molecule. Briefly, biotinylated fibrinogen was first diluted to 1 μM with 200 μL of 1× phosphate buffered saline (pH 7.4) + 0.1% Tween and then flowed across the surface of a SA sensor chip (Cytiva, USA) at a flow rate of 30 μL/min, reaching ~6400 response units (RU). All the binding experiments were performed at 25 °C at a continuous flow rate of 30 μL/min with 1× phosphate buffered saline (pH 7.4) + 0.1% tween +1% DMSO to maintain compound solubility. Due to the use of DMSO and its high refractive index contribution, solvent correction was applied, and signal corrected against the control surface response. Serial concentrations of the small molecules were run across the chip surface at 7.8125, 15.625, 31.25, 62.5, 125 and 250 μM. All the equilibrium constants (KDs) used for evaluating binding affinity were determined with Biacore Insight Evaluation Software (Cytiva, USA).

2.2. Experimental protocols

All participants provided written informed consent according to a protocol approved by Medicine and Health Regulatory agency (NRES-011NE to FDG, IRAS 15/NE/0211). The privacy rights of the human subjects have been observed. All SSc patients fulfilled the ACR/EULAR 2013 criteria [33]. Patients were included in an at-risk population if they presented with Raynaud's and any very early diagnosis of SSC (VEDOSS) criteria [34–36]. By definition, at-risk patients did not meet ACR/EULAR 2013 classification criteria for SSc (score < 9), neither did they fulfil classification for any other connective tissue disease.

2.2.1. Cell culture

Full thickness skin biopsies were surgically obtained from the forearms of three adult healthy controls (HC), three adult patients with recent onset SSc, defined as a disease duration of less than 18 months from the appearance of clinically detectable skin induration. All patients satisfied the 2013 ACR/EULAR criteria for the classification of SSc and had diffuse cutaneous clinical subset (dcSSc) as defined by LeRoy *et al.* [37], and 6 very early diagnosis of SSc (VEDOSS) patients. Fibroblasts were isolated from skin biopsies by expansion out of the cut biopsies, and primary cell lines established after two passages. Human telomerase-immortalisation was carried out using retroviral transduction as described [38,39]. Experimental testing on dermal fibroblast primary cell lines were performed within 10 passages. Cells were maintained in Dulbecco's modified Eagle medium (DMEM) (Gibco) supplemented with 10% FBS (Sigma) and penicillin-streptomycin (Sigma). TGF-β1 treatment (10 ng/ml) was used in 1% FBS conditions following an overnight starvation in 1% FBS.

2.2.2. Western blotting

Total proteins were extracted from fibroblasts in RIPA buffer and resolved by SDS-PAGE (10–15% Tris-Glycine). Proteins were transferred onto Hybond nitrocellulose membranes (Amersham biosciences) and probed with antibodies specific for TNC (Santa Cruz Biotechnology) and α-smooth muscle actin (Abcam) or loading control β-actin. Immunoblots were visualized with species-specific HRP conjugated secondary antibodies (Sigma) and ECL ThermoFisher Scientific (/Pierce) on a Biorad chemiDoc imaging system.

2.2.3. Quantitative real time PCR

RNA was extracted from cells using the RNA extraction kit (Zymo Research) following the manufacturing protocols. RNA was reverse transcribed using the cDNA synthesis kit (ThermoFisher Scientific). Q-RT-PCR were performed using SyBr Green PCR kit (ThermoFisher Scientific) with primers specific for *TNC* (Forward 5'-TCGACGTGTTTCCCAGACAG-3′; Reverse 5'-AACGGTGTCTTCCAGAGCAG-3′), *COL1A1*

(Forward; CCTCCAGGGCTCCAACGAG Reverse; TCTATCACTGTCTTGCCCCA), *COL1A2* (Forward; GATGTTGAACTTGTTGCTGAGC Reverse; TCTTTCCCCATTCATTTGTCTT), *ACTA2* (Forward; TGTATGTGGCTATCCAGGCG Reverse; AGAGTCCAGCACGATGCCAG), *CCN2* ((Forward; GTGTGCACTGCCAAAGATGGT Reverse; TTGGAAGGACTCACCGCT) and *GAPDH* (Forward; ACCCACTCCTCCACCTTTGA Reverse; CTGTTGCTGTAGCCAAATTCGT). The data obtained was analysed according to the ΔΔ Ct method. *GAPDH* served as housekeeping gene. Composite profibrotic score was calculated using the mean value of ΔΔ Ct of *COL1A1, COL1A2, ACTA2* and *CCN2* for each sample.

2.2.4. Collagen gel contraction assay

Collagen gel contraction assays were prepared using Cell Contraction Assay Kits (Cell Biolabs), per manufacturer instructions. Briefly, 2×10^5 fibroblasts were cultured within collagen gel for 16 h at 37 °C 5% CO2, then released from the sides of wells and photos taken over 48 h. The percentage change in gel area relative to area of gel at 0 h was analysed with ImageJ software.

2.2.5. Live dead cell assay

Fibroblasts were seeded at a density of 20,000 cells per well in a 24 well plate. Cells were treated with DMSO vehicle or small molecule (10 μM) for 24 h. Experiments were performed in triplicate. Cell viability was determined using LIVE/DEAD™ fluorometric assay according to the manufacturer's instructions (Invitrogen).

2.2.6. Statistical analysis

Categorical variables were presented as numbers and percentages, while continuous variables were reported as mean ± standard deviation (SD), mean ± standard error (SEM), or median with interquartile range (IQR) depending on the data distribution. Comparisons between groups were conducted using the student *t*-test or chi-square test. Statistical significance was defined as a *p*-value less than 0.05 for all analyses, and all tests were two-tailed. Data analysis was performed using RStudio (version 2023.03.0) or GraphPad Prism software (version 9.5.1).

3. Results

3.1. TNC mRNA and protein levels elevated in SSc and VEDOSS dermal fibroblasts correlates to levels of profibrotic gene expression

TNC gene expression was observed to be higher in fibroblasts isolated from SSc patients as well as in fibroblast from VEDOSS patients, being approximately 7-fold and 5.5-fold greater than HC levels for SSc and VEDOSS respectively (Fig. 1A), however due to heterogeneity in the different donor SSc fibroblast cell lines, this did not reach significance. When assessing the profibrotic gene expression of the biological triplicates of HC and SSc dermal fibroblast cell lines, by assessing mRNA

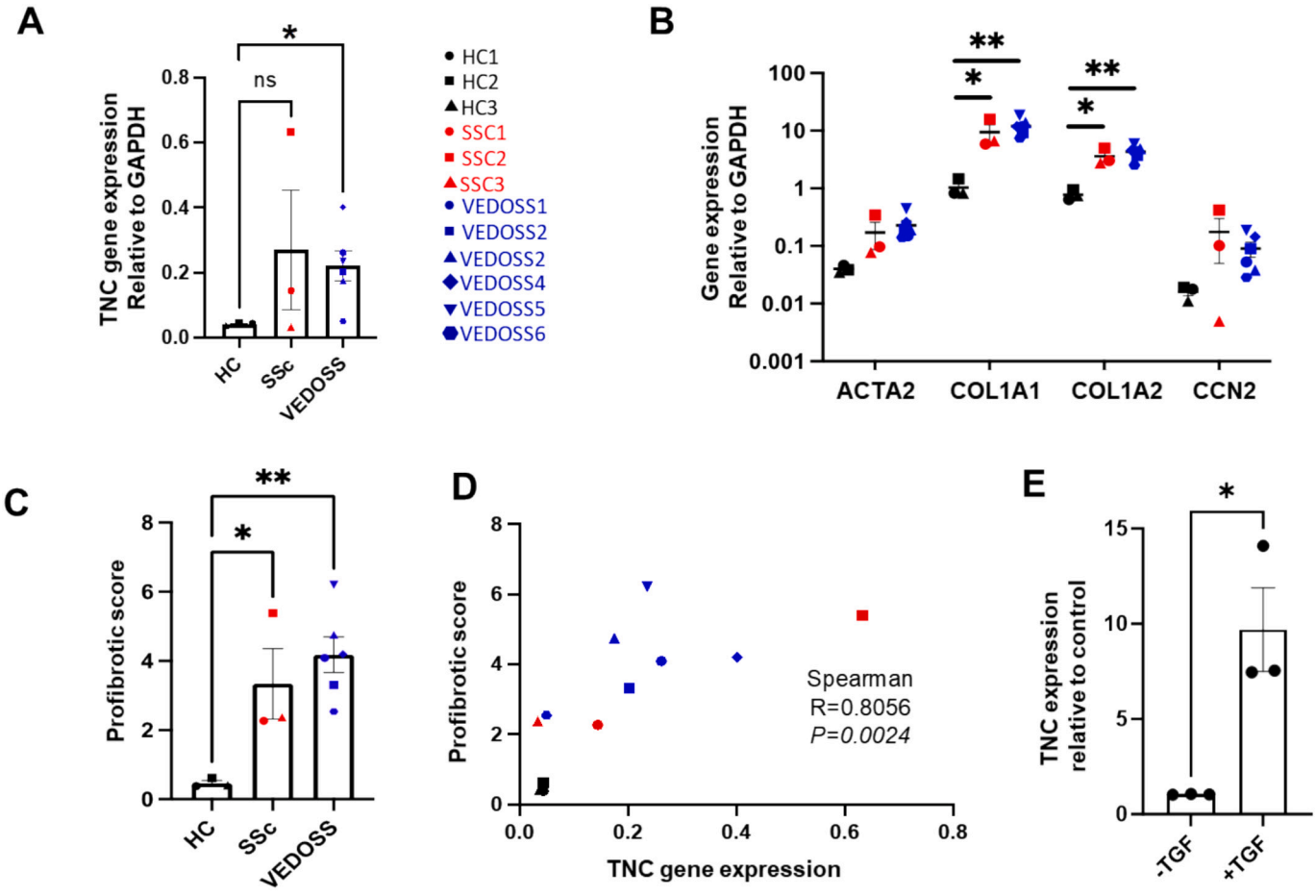

Fig. 1. TNC expression in dermal fibroblasts correlates to levels of profibrotic markers. TNC mRNA expression in HC (*n*=3), SSc (n=3) and VEDOSS (*n*=6) fibroblasts in starved conditions **(A)**. Each symbol represents a cell line generated from a single donor (HC; Black, SSc; Red, VEDOSS; Blue). Gene expression analysis for *ACTA2, COL1A1, COL1A2, CCN2* relative to housekeeping gene *GAPDH* for all dermal fibroblast cells line in A **(B)**. Combination of analysis from B into a profibrotic score for each category of dermal fibroblast **(C)**. Correlation between TNC gene expression and profibrotic score for data in B and C **(D)**. TNC mRNA expression in HC dermal fibroblasts (*n*=3) with and without TGF-β1 **(E).** Bar charts represent mean ± standard error (SE). Statistical tests used; unpaired student *t*-test (two tailed) (A, B, C and E) and spearman correlation (D). Statistical significance illustrated; * =$P<0.05$, ** =$P<0.01$ and ns = non-significant. (For interpretation of the references to colour in this figure legend, the reader is referred to the web version of this article.)

levels of *CCN2, COL1A1, COL1A2*, and *ACTA2*, all SSc fibroblasts samples collectively showed increased gene expression compared to HC, with significant differences observed with *COL1A1* and *COL1A2* (Fig. 1B). Combining these genes into a profibrotic score shows SSc fibroblasts have an increased level compared to HC (Fig. 1C). Interestingly, there is a strong correlation with the profibrotic score and TNC gene expression in all fibroblasts cell lines, showing a direct link between the fibrotic phenotype of SSc dermal fibroblasts and TNC expression (Fig. 1D). Moreover, all single genes show strong correlation with TNC expression (Spearman Correlation $R > 0.7986$, $P < 0.0027$), with *CCN2* showing the strongest correlation ($R = 0.9142$ $P < 0.0001$). Moreover, the SSC3 cell line with low basal TNC expression, had the lowest *CCN2* expression (Fig. 1B and C) which is in line with previous studies that demonstrate an induction of TNC following CCN2 stimulation [40–42]. We also demonstrate that TNC expression is enhanced by profibrotic cytokine, TGF-β1, in HC dermal fibroblasts (Fig. 1E). TGF-β1 stimulation of 24 h triggered an increase in fibroblast TNC expression by 6-fold (Fig. 1E). This is consistent with the observations of Bhattacharyya who demonstrated a dose- and time-dependent TGF-β-induced upregulation of TNC in both neonatal and adult skin fibroblasts [4].

3.2. Adhiron guided small molecule identification

3.2.1. Identification and isolation of Adhiron with inhibitory properties

Adhirons have been previously shown to bind to 'hot spots' on protein surfaces blocking protein function through steric and allosteric mechanisms [18,21,22,43]. Here we determined the ability to isolate Adhirons capable of blocking the interaction of the FBG domain of TNC (FBG—C) with TLR4. The BAP tag labelled FBG-C domain was expressed in shuffle cells and purified using a two-step purification method (**Supplementary Fig. S1A**). *In vivo* biotinylation of the FBG-C domain allowed isolation of Adhiron reagents by phage display. Biotinylation was confirmed by western blotting (**Supplementary Fig. S1B**). The purified bap tagged FBG-C domain was panned against the Adhiron phage library [16,28,44]. After three panning round 96 clones were picked and assessed using phage ELISA [28] (**Supplementary Fig. S2**).

Seven out of the 96 Adhirons were non-specific as they interacted with both FBG-C domain and the control (**Supplementary Fig. S2**). DNA sequencing highlighted a consensus motif on variable region 1 across the 86 clones. Due to factors such as expression yields, solubility, and stability, six Adhirons were taken forward for further characterisation (Fig. 2A). The six Adhirons were subcloned into pET11a, expressed in BL21 DE3 star cells and purified. The Adhirons were tested for the ability to block the TLR4/FBG-C interaction. The solid phase inhibition assay showed that as expected the scaffold (control Adhiron) did not inhibit the TLR4/FBG-C interaction. At the same concentrations, Adhirons 9, 12, 32, 45 and 52 showed different degrees of inhibition whereas Adhiron 47 did not inhibit (Fig. 2D). Variable region 1 of Adhiron 47 did not have the conserved motif like Adhirons 9, 12, 32, 45 and 52 suggesting that Adhiron 47 may have a different epitope

Table 1
Adhiron loop sequences.

Adhiron	Variable Region 1	Variable Region 2
9	PVNP**HQWAD**	YTRFQEVAR
12	ESNPHMW**AD**	WTVRNNRMA
32	EANQ**HFYAD**	WQINQGIIF
45	MTQP**HRNAD**	YYRNLHGIY
47	VFFMQWEHH	GHQRHAHYA
52	GANM**HAYAD**	WEMSRKLMT
Scaffold	AAAA	AAE

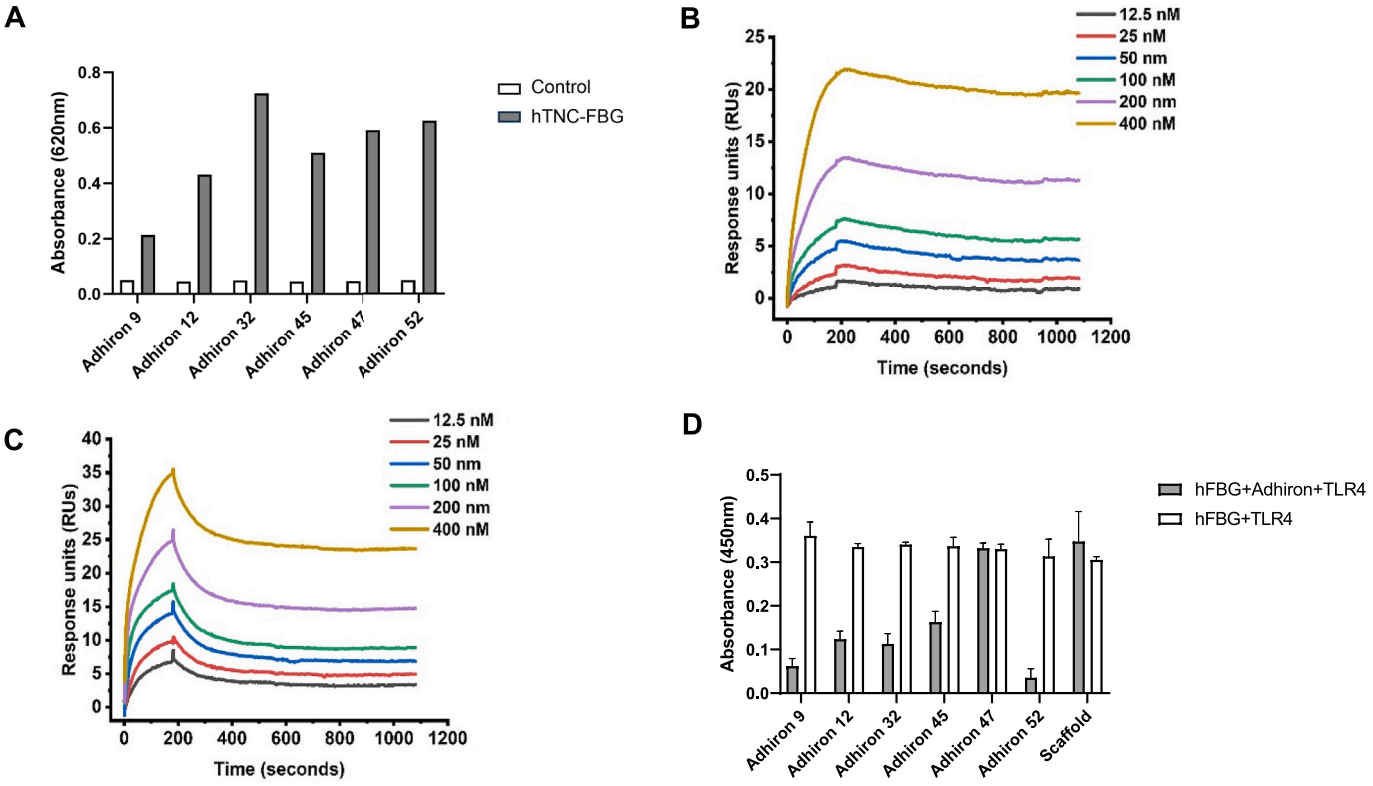

Fig. 2. Phage ELISA and solid phase inhibition assay: Phage ELISA results of 6 candidate Adhirons identified in screens against the FBG domain of human TNC (hTNC-FBG) **(A)**. Kinetic analysis of Adhiron 52 binding to human **(B)** and mouse **(C)** FBG-C by surface plasmon resonance (SPR). Representative sensorgram obtained from injection of Adhiron at concentrations of 12.5, 25, 50, 100, 200 and 400 nM. Solid phase inhibition assay. 96-well plates coated with 5 μg mL^{-1} of FBG-C (Human) were incubated with TLR4 only (white) and TLR4 in the presence of Adhiron (grey). Data are shown as mean ± SEM, n=3 **(D)**.

compared to other Adhirons (Table 1). The solid phase inhibition assays showed that Adhiron 52 displayed the best inhibition (Fig. 2D) and SPR indicated binding affinities of 15.3 nM and 11.8 nM for human and mouse FBG—C, respectively (Fig. 2B, C).

3.2.2. *Structural insights into Adhiron 52 and FBG-C domain interaction*

To gain atomic insights into how Adhiron 52 interacts with FBG-C domain, the Adhiron/FBG-C complex was produced and crystallised (PDB ID 9R5Y, **Supplementary Fig. S1C and D**) in space group P21 21 21 with two complexes in the asymmetric unit. The structure was determined by molecular replacement and refined at resolution 1.4 Angstroms (**Supplementary Table S1**). In complex with Adhiron 52, the overall structure of the FBG-C domain does not change. It maintains the three subdomain ABP structure observed in FRePs (Fig. 3A). Adhiron 52 interacts with the FBG-C at the p subdomain (Fig. 3A). However, in comparison to uncomplexed FBG-C domain (PDB6QNV), the Adhiron results in subtle changes in the cation ridge region, the proposed TLR4 binding site [30]. On interaction with the Adhiron, part of the cationic ridge β - strand becomes less structured and the side chains of residues E2104 and V2103 take up different conformations (Fig. 3B). Moreover, the disordered binding loop due to the absence of Ca^{2+} observed in FBG-C structure (PDB - 6QNV) is structured in Adhiron/FBG-C complex indicating that Adhiron 52 stabilises the disordered Ca^{2+} binding loop in the absence of calcium (Fig. 3B).

The crystal structure showed that variable region 1 on Adhiron 52 forms the major contact site with residues G39, N41, H43, Y45 and D47 involved in hydrogen bonds with residues H2175, H2150, S2164, Y2140, N2148 and Y2116 in subdomain P of FBG-C (Fig. 4, inserts 1, 2 and 3). The main chain carbonyl group of G39 interacts with a hydrogen donated by a nitrogen on the imidazole group of H2175. N41 forms a hydrogen bond network where the side chain amide group interacts with the side chain hydroxyl group of S2164 while side chain carbonyl group interacts with backbone amide group of H2150. The imidazole group nitrogen atoms on H43 interact with hydroxyl group of Y2140 and the side chain carbonyl group of N2148 through hydrogen acceptor (N···H-O) and hydrogen donation (N-H···O) respectively. Simultaneously, the side chain amide group of N2148 interacts with the main chain carbonyl group of Adhiron residue Y45. Adhiron residue D47 forms the final hydrogen bond network with residues Y2116 and Adhiron residue W73. The side chain hydroxyl group of D47 interacts with Y2116 while the carbonyl group interacts with the main chain amide group of Adhiron residue W73 also forms a hydrogen bond. Fewer hydrogen bonds were observed in the variable region 2 of the Adhiron 52 and FBG-C interaction interface (Fig. 4). A water molecule acts as a bridge between Adhiron residue E74 and FBG-C residue R2147 (Fig. 4, insert 6). Adhiron residues, Y43, W73, M75 and M80 stack against each other to form a hydrophobic pocket which I2133 on FBG-C snugly fits in (Fig. 4, insert 5) and stabilises the disordered Ca^{2+} binding loop. The main chain amide group of residue M75 interacts with the carbonyl backbone group of FBG-C residue S2131 further increasing the stability of the disordered loop in the absence of calcium.

Finally, a lack of cross reactivity of Adhiron 52 with other members of the Tenascin family, notably, Tenascin R and Tenascin X was demonstrated (**Supplementary Fig. S3 and S4**).

3.2.3. *Identification of small molecules to mimic Adhiron 52*

Three amino acid residues were found to be crucial for the Adhiron-FBG-C interaction: N41, H43 and D47. We used the ligand-based

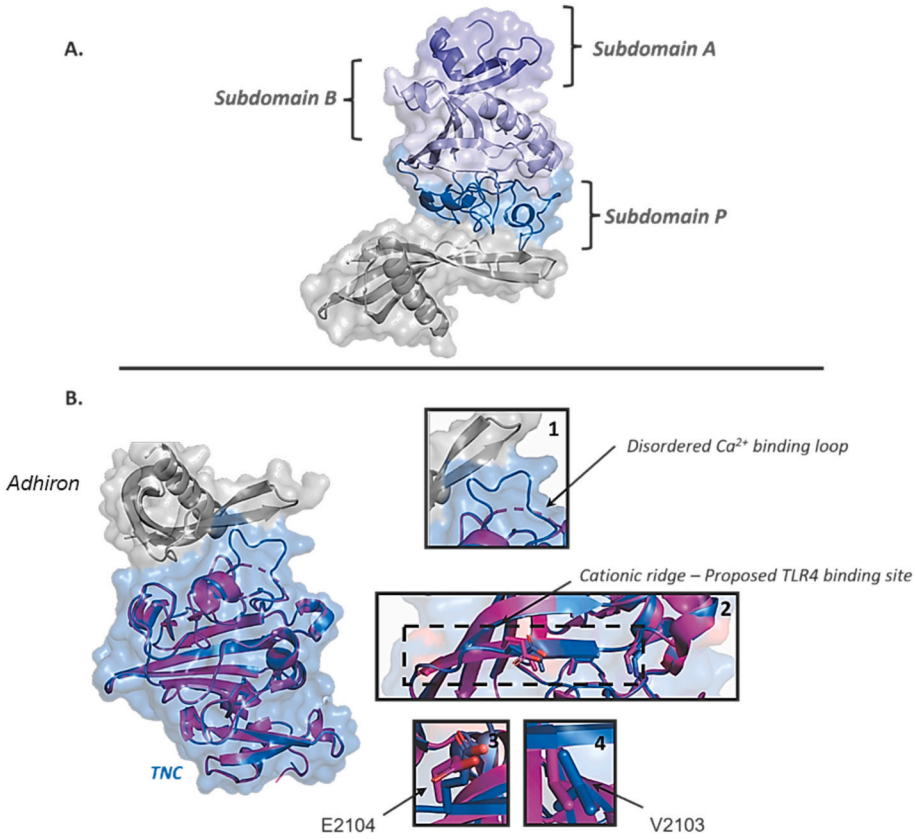

Fig. 3. The crystal structure of Adhiron 52/FBG-C complex. A) The different shades of blue show the ABP subdomains. Subdomain A is shown in slate, subdomain B in light blue and subdomain P in sky-blue **(A)**. Structural alignment of FBG-C/Adhiron 52 complex (Skyblue; PDB: 9R5Y) with non-complexed FBG-C (Magenta; PDB: 6QNV). *Insert 1* shows the structural changes in the disordered Ca^{2+} binding loop. *Insert 2* displays the subtle changes to the TLR4 binding site (cationic ridge). *Inserts 3 and 4* show conformational changes of residues E2104 and V2103 (**B**). (For interpretation of the references to colour in this figure legend, the reader is referred to the web version of this article.)

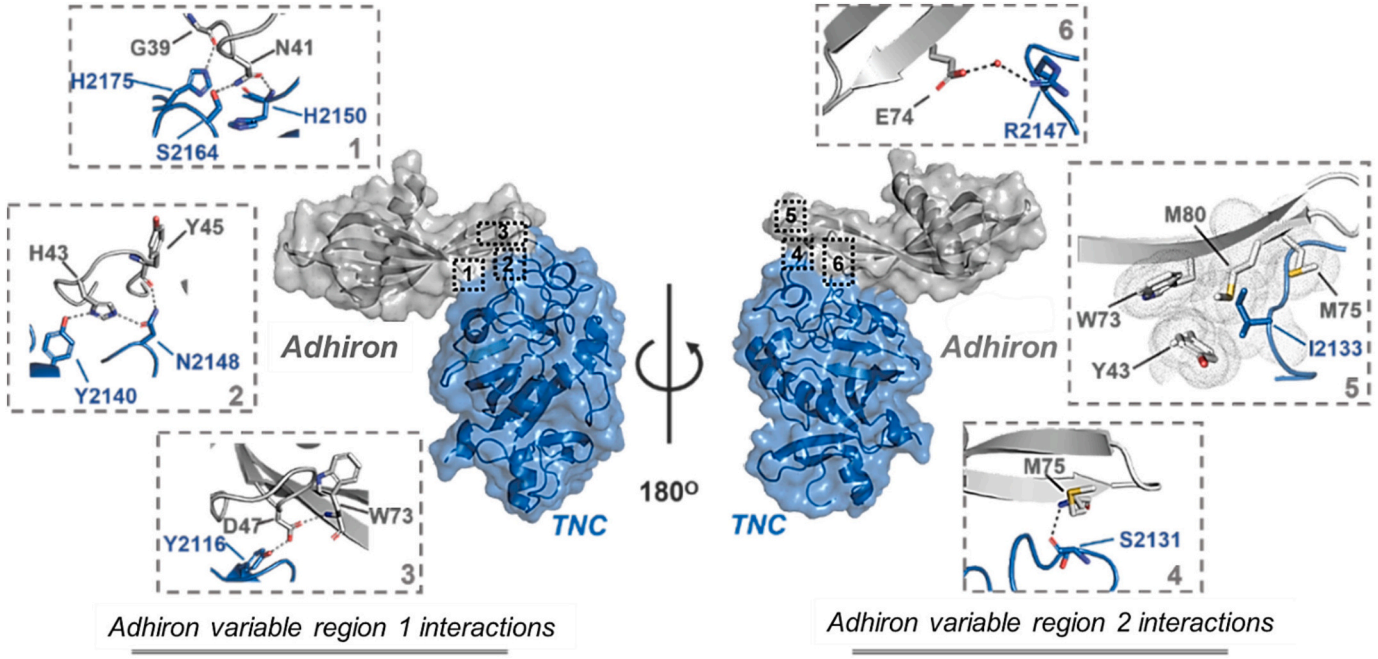

Fig. 4. The crystal structure of FBG domain of human TNC (Skyblue) bound to Adhiron 52 (grey) (PDB: 9R5Y) inserts 1–3. show how five residues on the variable loop 1 of Adhiron 52 (G39, N41, H43, Y45 and D47) interact with six residues on hFBG (Y2116, Y2140, N2148, H2150, S2164 and H2175). Inserts 4–6 show the interactions between variable loop2 and FBG-C domain. Adhiron residues E74, Y43, W73, M80 and M75 interact with residues R2174, I2133 and S2131 on FBG-C. (For interpretation of the references to colour in this figure legend, the reader is referred to the web version of this article.)

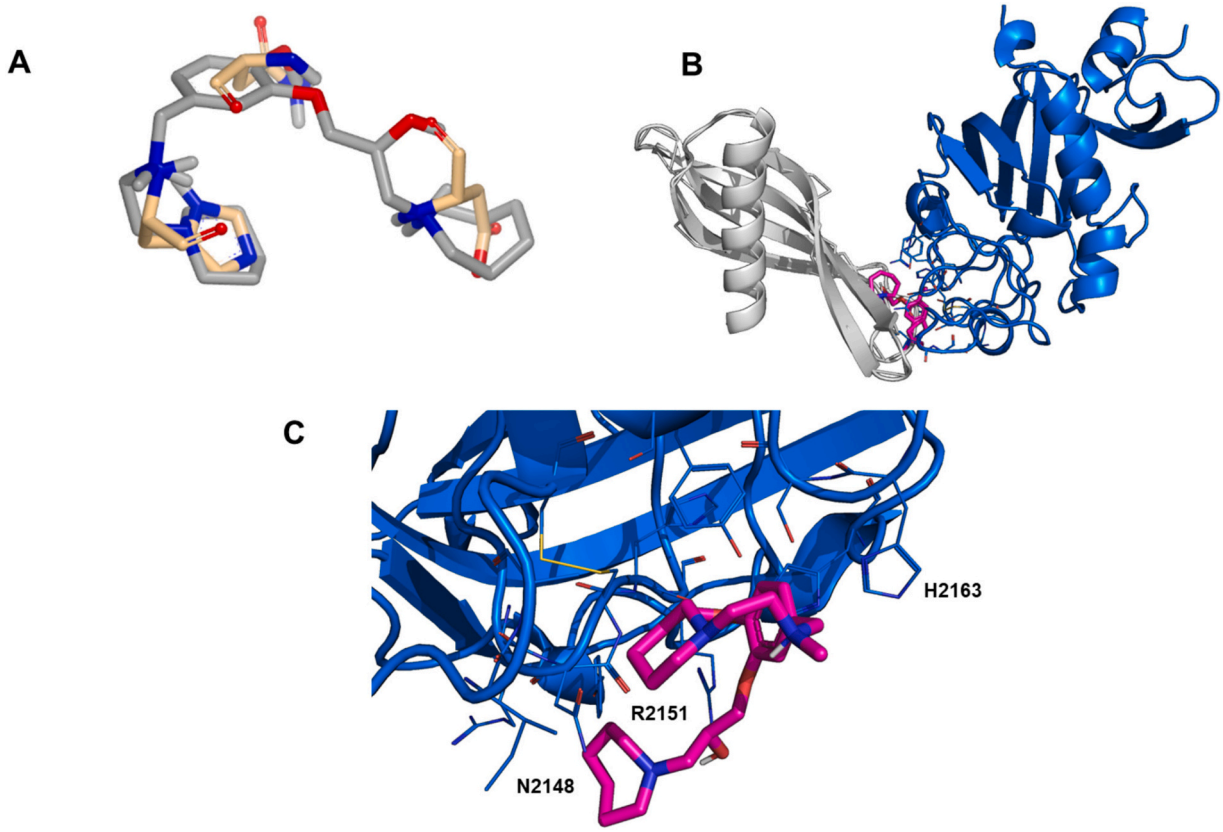

Fig. 5. Identification of compounds as mimics of Adhiron 52. Small molecule 830 (grey sticks) mimics the shape and electrostatic interaction of Asn41 and His43 from Adhiron loop1 (beige sticks) **(A)**. Adhiron (grey ribbons) bound to FBG domain of TNC (blue ribbons) with predicted binding mode of 830 shown as pink sticks **(B).** Close up of predicted binding mode of 830 with the FBG domain of TNC **(C).** (For interpretation of the references to colour in this figure legend, the reader is referred to the web version of this article.)

screening tool ROCS and identified compounds from the eMolecules library which mimicked the shape and electrostatic interactions of the key amino acid residues from Adhiron 52 (Fig. 5A-C). Ten hit compounds were purchased **(Supplementary Table S2)** and their integrity was checked by LCMS before *in vitro* evaluation.

3.3. Targeting FBG-C domain with small molecules reduces the profibrotic phenotype of human dermal fibroblasts

To test the ability of the small molecules, to modulate the interaction of the FBG-C domain of Tenascin C with TLR4, we measured their ability to reduce profibrotic responses in healthy human (HC) dermal fibroblasts. Cell lines were treated for 24 h with 10 μM of each small molecule along with the profibrotic cytokine, TGF-β1, and the combined gene expression (expressed as a profibrotic score) of the profibrotic genes αSMA, COL1A1, COL1A2 and CCN2 was compared relative to that induced by TGF-β1 and DMSO vehicle (control, CTR) only (Fig. 6A). Two molecules; 464 (49306**464**) and 830 (73494**830**) reduced the TGF-β1-induced profibrotic score relative to TGF-β1 (Fig. 6A, B). These had no effect on cell viability as assessed using a Live/Dead cell assay (Thermo Fisher Scientific, **(**Fig. 6C**)**. Both these molecules displayed structural similarity and the dissociation constant of 830 was measured at 553 μM **(**Fig. 6D**)**.

Early stage physicochemical profiling of 464 and 830 to ascertain metabolic stability and aqueous solubility of the molecules *in vitro* demonstrated that both molecules displayed good solubility (>75 μM) and human liver microsomal stability (clearance of 5-10 μL/min/mg) **(**Table 2**)**.

Due to the specific binding affinities of 830 to the FBG domain of TNC (Fig. 6D) and the structural similarity between 464 and 830, both these inhibitors were retested on dermal fibroblast isolated from SSc patients, where they were shown to reduce the composite pro-fibrotic gene score back to control unstimulated levels (Fig. 7A). Moreover, an attenuation of the TGF-β1 induced fibrotic response by the selected inhibitors was further demonstrated in collagen gel contraction assays using HC dermal fibroblasts. With 2 h of TGF-β1 stimulation, a significant gel contraction was induced, since gel area contracted to 85% of 0 h condition compared to CTR (97%) (Fig. 7B-C). Treatment with inhibitor 464 (94%) and 830 (91%) were able to reduce TGF-β1 triggered gel contraction to that not significantly different to CTR levels (97%) compared to 0 h timepoint (Fig. 7B-C).

Whilst the binding affinity measured using SPR is lower than may be expected from the results of the cellular assays, there may be a number of reasons for this. The biotinylated FBG domain of TNC may be immobilised in a conformation that is not that found *in vivo* leading to the lower than expected affinity based on our cellular assays.

Table 2
Early stage physicochemical profiling of 464 and 830.

Compound ID	Aqueous Solubility μM (pH 7.4)	Microsomal stability (human) CL_{int} (μL/min/ mg protein)
464 - (49306464)	>100	<8.6
830 - (73494830)	75	5

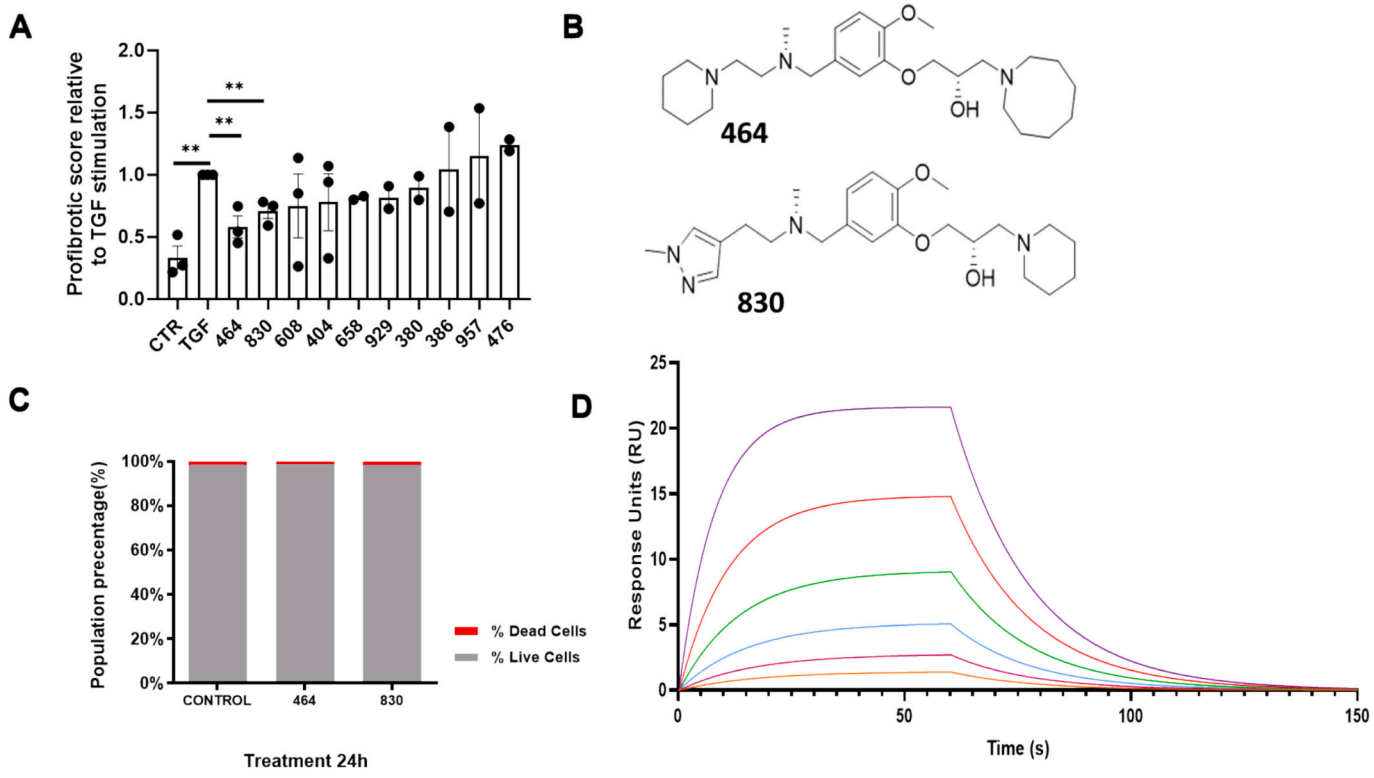

Fig. 6. The properties of the lead candidate molecules (464, and 830) on fibrosis, cell viability and FBG-C binding. The effect of inhibitors on TGF-β1 induced profibrotic score of human dermal fibroblasts. Healthy dermal fibroblasts (n = 2–3, each symbol represents a cell line generated from a single donor) treated with DMSO vehicle or inhibitors in TGF-β1 conditions for 24 h, as well as control (CTR) conditions. Gene expression of *ACTA2, COL1A1, COL1A2* and *CCN2* relative to *GAPDH* analysed and combined into a profibrotic composite score relative to that induced in TGF-β1 + DMSO only (TGF) condition **(A).** Chemical structure of molecules 464 and 830 **(B)**. Effect of small molecule 464 and 830 (10 μM, 24 h) on fibroblast viability using a Live/Dead cell assay **(C).** Kinetic analysis of 830 binding to FBG-BAP using surface plasmon resonance (SPR) technology. Representative sensorgram of dose response obtained from injection of 830 at concentrations of 7.8125, 15.625, 31.25, 62.5, 125 and 250 μM. Mean Kd of 533 μM (n=3) **(D).**

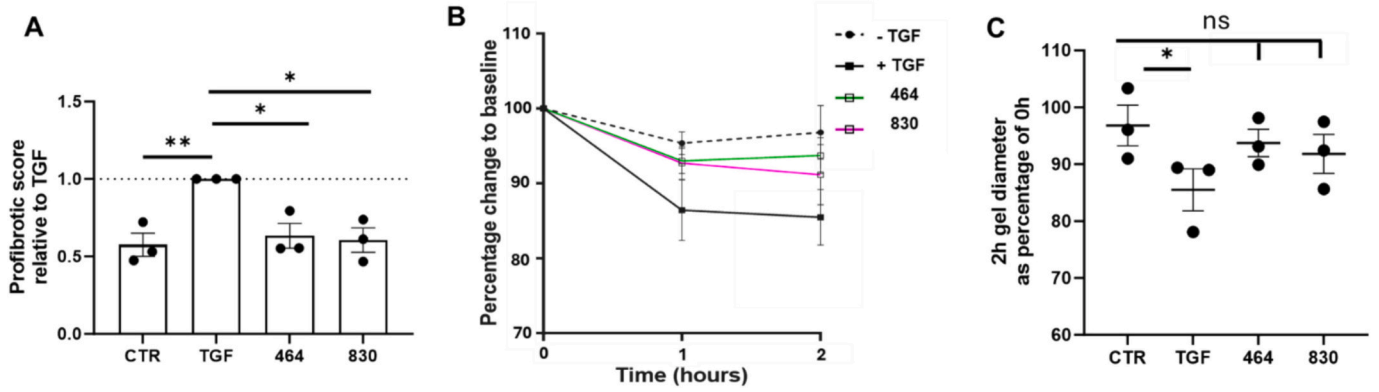

Fig. 7. FBG-C targeting by 464 and 830 reduces the TGF-β1 induced profibrotic phenotype of human dermal fibroblasts. Reduced subset of inhibitors was tested on SSc dermal fibroblasts (n=3) and fibrotic score analysed as in Fig. 7 (above) **(A).** Percentage change in gel contraction of gel cultured with healthy fibroblasts over 2 h compared to baseline area (0 h). Cells were treated with TGF-β1 and DMSO (+TGF), or inhibitor (464 or 830) or in control conditions (-TGF) **(B-C)**.

4. Discussion and conclusion

4.1. Tenascin-C levels are increased in tissue of patients with SSc and correlate with markers of fibrosis

Constitutive production of TNC was observed in dermal fibroblasts isolated from patients with SSc compared to healthy controls. This is consistent with the current data and previous clinical observations associating high circulating TNC levels with markers of SSc and implies that the increased TNC accumulation may result from its cell autonomous overproduction by activated fibroblasts [4] (Fig. 1A). Increased expression of TNC was also correlated with an increase in fibrotic gene score, notably ACTA2, COL1A1, COLl1A2 and CCN2 (Fig. 1B-D), which are key molecular markers that are significantly and reliably upregulated by TGF-β and represent different, interconnected, aspects of the fibrotic process [45–47]. TNC has been reported to elicit cell specific responses including type 1 collagen synthesis where it drives the fibrotic response in dermal and lung fibroblasts and contributes to the integrity of the ECM in young skin [4,48]. Moreover, TNC silencing results in the reduction of CCN2 in the kidney mesangial cells [49] and reciprocally CCN2 promotes deposition of several ECM proteins, including collagen, fibronectin and TNC [50]. Interestingly, we report for the first time that TNC expression is also raised in dermal fibroblasts isolated from VEDOSS individuals (Fig. 1A), which have been characterised previously to show biomarkers seen in SSc fibroblasts, although from sites of absent clinical fibrosis [39]. Studies have reported a potential role for TNC in the early diagnosis of rheumatoid arthritis (RA), where the detection of antibodies to citrullinated TNC in patients with early synovitis was associated with the development of RA [51]. The early detection of TNC in dermal fibroblasts biopsies of VEDOSS patients might offer similar opportunities in identifying individuals at risk of developing SSc.

4.2. Tenascin C expression is induced by the profibrotic cytokine TGF-β

We demonstrated that TNC expression in HC fibroblasts is induced by the profibrotic cytokine TGF-β, this is consistent with earlier reports by Bhattacharyya *et al.* who also suggested that autonomous TNC upregulation by fibroblasts in various fibrotic disorders maybe due to autocrine stimulation by TGF-β [4]. TGF-β has been identified as a regulator of pathological fibrogenesis in SSc and related fibrotic disorders. Dysregulation of TGF-β signalling is evident in SSc and high levels of this profibrotic cytokine and its regulated genes have been detected in skin biopsies, being positively correlated with the severity of the disease [4]. Although the inhibition of TGF-β, has been demonstrated as an efficient strategy for reducing fibrosis in preclinical models, translating these findings into clinic has proved difficult due to adverse effects stemming from TGF-β's physiological actions in inflammation and tissue homeostasis. Fresolimumab, a TGF-β neutralizing antibody, does exert antifibrotic effects in SSc patients, though this is accompanied by a high incidence of keratoacanthomas, which limits its use in treatment [52]. Consequentially, alternative treatments are being sought.

TGF-β increases TNC expression in cardiac [53], lung [54], intestinal subepithelial [55] and dermal fibroblast [4]. The latter was supported by our current observations, which demonstrated a 3 and 5 fold increase in TNC expression for SSc and HC fibroblasts, respectively. Previous evidence that TGF-β Receptor Kinase inhibitor SB-431542, abolished the induction of TNC by TGF-β and that TGF-β failed to induce TNC expression in Smad3$^{-/-}$ fibroblasts support a role for TGF-β signalling in TNC induction [4].

It is noteworthy that TNC deficiency attenuates TGF-β-mediated fibrosis in both isolated dermal and lung fibroblasts. TGF-β stimulation of type 1 collagen and αSMA was attenuated in fibroblast isolated from TNC$^{-/-}$ null mice compared to wild type fibroblasts [4,6]. TNC deficiency also attenuated TGF-β-mediated fibrosis following murine lung injury [6]. TNC-null mice had 85% less lung collagen than wild-type mice, following bleomycin injury (which is dependent on canonical TGF-β signalling), with the lung interstitium containing fewer myofibroblastsand cells with intranuclear Smad-2/3 staining, suggesting impaired TGF-β activation or signalling [6] and implying a role for TNC in TGF-β's fibrotic response.

Recently a role for TLR4 signalling in the augmentation of TGF-β responses in SSc was proposed [45]. Elevated expression of TLR4, together with increased accumulation of endogenous TLR4 ligands (notably TNC, fibronectin-EDA and hyaluronic acid), in lesional skin and lung tissues from patients with SSc and in mice with bleomycin-induced SSc was reported [56]. Moreover, TLR4 activation also induced stimulation of ECM gene expression in explanted skin fibroblasts and significantly enhanced their ability to mount a profibrotic response when challenged with TGF-β1. A model for fibrogenesis was thus proposed whereby tissue damage resulting from chronic injury stimulates the local generation and accumulation of TNC, this then activates TLR4 signalling in resident fibroblasts resulting in enhanced ECM production and TGF-β secretion and a self-amplifying vicious cycle of fibrosis [9] (Fig. 8). Targeting the TNC-TLR4 interaction represents a promising anti-fibrotic therapy. However, targeting TLR4 directly to break this feedback loop may compromise the host immune defence. Disrupting persistent TLR4 signalling by targeting the endogenous ligand's, notably TNC, interaction with TLR4, does however, represents a potential novel strategy for breaking the cycle of progressive fibrosis in SSc [4,9].

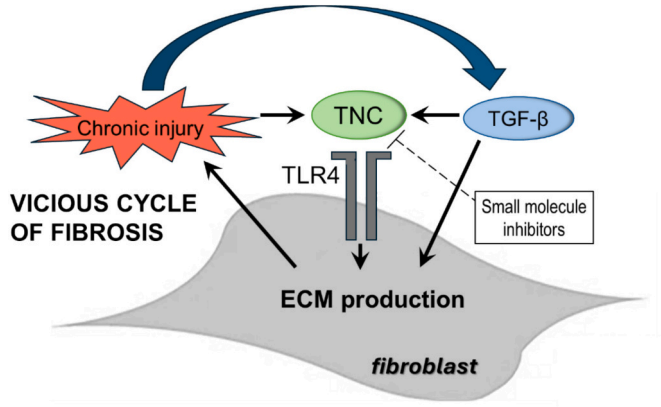

Fig. 8. Mechanism of self-sustaining fibroblast activity and fibrosis in SSc, whereby tissue injury and TGF-β induce TNC expression resulting in the activation of TLR4 causing further tissue damage and ECM production. Adapted from [9,57].

4.3. Small molecule modulators of the interaction between to the FBG domain of TNC and TLR4 can attenuate TGF-β induced fibrotic responses

We demonstrate that small molecule inhibitors 464 and 830 that target the FBG domain of TNC to block its interaction with TLR4, were able to attenuate the profibrotic effects of TGF-β. These inhibitors were designed using an Adhiron guided ligand discovery technique. Small molecules were selected based on their ability to mimic the structure of the interacting residues from the Adhiron that binds to FBG and prevents its interaction with TLR4. Specific binding of the selected inhibitors to the FBG domain was confirmed using SPR. Adhiron reagents are small non-antibody binding proteins that have been used in broad applications including in the modulation of protein function and protein–protein interactions. Although, their use in multiple protein capture-based assays (immunoassays and diagnostics) has been established, *in vivo* therapeutic application is at present in its early stages, hence the interest in developing a series of small molecule to mimics their effect.

Both 464 and 830 have structural similarity (Fig. 6B) in that they both contain the same central substituted dimethoxyphenyl core, however 464 contains a saturated piperidine ring on the western portion of the molecule whereas 830 contains an aromatic *N*-methylpyrazole. The eastern portion of the molecules both contain saturated ring systems, with 830 having a piperidine whereas 464 contains the larger azapane ring. Importantly both inhibitors display favourable ADME properties making them suitable for further optimisation (Table 2). While the preliminary ADME profiles of these molecules are encouraging, they require further iterative rounds of optimisation to achieve comparable efficacy and pharmacological properties to established anti-fibrotic agents such as pirfenidone and nintedanib. However, both of these drugs are associated with adverse effects including nausea, diarrhoea, and weight loss, highlighting the ongoing need for the development of novel therapeutic options. Both inhibitors were effective in reducing the expression of TGF-β stimulated fibrotic genes including αSMA, COL1A1, COL1A2 and CCN2 as well as myofibroblast differentiation as assessed by attenuation of collagen gel contraction. In conclusion, these finding indicate that small molecules selectively targeting the interaction of the FBG domain of TNC with TLR4 abrogated fibrotic responses in SSc fibroblasts *in vitro* following TGF-β stimulation, with 464 and 830 being promising candidates for further development as anti-fibrotic drugs. Moreover, it highlights the utility of Adhiron guided ligand discovery to generate small molecule inhibitors to selectively target protein-protein interactions.

Limitations of the study: This proof-of-concept study has identified first-generation compounds that effectively suppress the profibrotic phenotype of dermal fibroblasts derived from patients with SSc. To validate the therapeutic potential of these compounds in a physiologically relevant context, further studies employing optimized second- or third-generation molecules in animal models of fibrosis as well as in immune cells (*e.g.* macrophages and dendritic cells), which have been implicated in the pathogenesis of SSc and in which TNC has been shown to function as an endogenous ligand for TLR4, are warranted. However, such investigations fall outside the scope of the current study. Additionally, it is acknowledged that our experimental approach relies on the indirect activation of the TNC-TLR4 signalling axis *via* TGF-β stimulation, rather than directly targeting the TNC–TLR4 interaction. Direct modulation of this pathway would be necessary to conclusively validate the mechanistic inferences drawn from our findings.

CRediT authorship contribution statement

Thembaninkosi Gaule: Writing – review & editing, Methodology, Investigation, Data curation. **Katie J. Simmons:** Writing – review & editing, Supervision, Methodology, Investigation, Data curation. **Kieran Walker:** Investigation, Data curation. **Francesco Del Galdo:** Writing – review & editing. **Rebecca L. Ross:** Writing – review & editing, Supervision, Methodology, Investigation, Data curation. **Hema Viswambharan:** Investigation, Data curation. **Jahnavi Krishnappa:** Investigation. **Jack Pacey:** Investigation. **Martin McPhillie:** Supervision, Investigation. **Darren C. Tomlinson:** Supervision, Methodology, Investigation, Funding acquisition, Data curation. **Azhar Maqbool:** Writing – review & editing, Writing – original draft, Project administration, Methodology, Investigation, Funding acquisition, Data curation, Conceptualization.

Declaration of competing interest

The authors declare that they have no known competing financial interests or personal relationships with other people or organisations that could be construed as influencing the work reported in this paper.

Acknowledgements

This work was supported by the British Heart Foundation Project Grant No: PG/17/72/33255. Biosample collection was funded by SRUK grant and Kennedy Trust Program Foundation Grant and supported by National Institute for Health and Care Research Biomedical Research Centre (NIHR BRC) (NIHR213331) and the Susan Cheney Scleroderma Research Foundation, the Medical Research Council (MR/S001530/1) (RR, FDG, KW).

Appendix A. Supplementary data

Supplementary data to this article can be found online at https://doi.org/10.1016/j.bioorg.2025.109251.

Data availability

Data will be made available on request.

References

[1] D.P. Tashkin, M.D. Roth, P.J. Clements, D.E. Furst, D. Khanna, E.C. Kleerup, J. Goldin, E. Arriola, E.R. Volkmann, S. Kafaja, R. Silver, V. Steen, C. Strange, R. Wise, F. Wigley, M. Mayes, D.J. Riley, S. Hussain, S. Assassi, V.M. Hsu, B. Patel, K. Phillips, F. Martinez, J. Golden, M.K. Connolly, J. Varga, J. Dematte, M. E. Hinchcliff, A. Fischer, J. Swigris, R. Meehan, A. Theodore, R. Simms, S. Volkov, D.E. Schraufnagel, M.B. Scholand, T. Frech, J.A. Molitor, K. Highland, C.A. Read, M.J. Fritzler, G.H.J. Kim, C.H. Tseng, R.M. Elashoff, Sclerodema Lung Study II Investigators. Mycophenolate mofetil versus oral cyclophosphamide in scleroderma-related interstitial lung disease (SLS II): a randomised controlled, double-blind, parallel group trial, Lancet Respir. Med. 4 (2016) 708–719, https://doi.org/10.1016/S2213-2600(16)30152-7.

[2] J.E. Pope, N. Bellamy, J.R. Seibold, M. Baron, M. Ellman, S. Carette, C.D. Smith, I. M. Chalmers, P. Hong, D. O'Hanlon, E. Kaminska, J. Markland, J. Sibley,

L. Catoggio, D.E. Furst, A randomized, controlled trial of methotrexate versus placebo in early diffuse scleroderma, Arthritis Rheum. 44 (2001) 1351–1358, https://doi.org/10.1002/1529-0131(200106)44:6<1351::AID-ART227>3.0.CO;2-I.

[3] O. Distler, K.B. Highland, M. Gahlemann, A. Azuma, A. Fischer, M.D. Mayes, G. Raghu, W. Sauter, M. Girard, M. Alves, E. Clerisme-Beaty, S. Stowasser, K. Tetzlaff, M. Kuwana, T.M. Maher, SENSCIS trial investigators. Nintedanib for systemic sclerosis-associated interstitial lung disease, N. Engl. J. Med. 380 (2019) 2518–2528, https://doi.org/10.1056/NEJMoa1903076.

[4] S. Bhattacharyya, W. Wang, L. Morales-Nebreda, G. Feng, M. Wu, X. Zhou, R. Lafyatis, J. Lee, M. Hinchcliff, C. Feghali-Bostwick, K. Lakota, G.R. Budinger, K. Raparia, Z. Tamaki, J. Varga, Tenascin-C drives persistence of organ fibrosis, Nat. Commun. 7 (2016) 11703, https://doi.org/10.1038/ncomms11703.

[5] K.E.N. Clark, E. Csomor, C. Campochiaro, N. Galwey, K. Nevin, M.A. Morse, Y. V. Teo, J. Freudenberg, V.H. Ong, E. Derrett-Smith, N. Wisniacki, S.M. Flint, C. P. Denton, Integrated analysis of dermal blister fluid proteomics and genome-wide skin gene expression in systemic sclerosis: an observational study, Lancet Rheumatol. 4 (2022), https://doi.org/10.1016/S2665-9913(22)00094-7, 0 e507-e516.

[6] W.A. Carey, G.D. Taylor, W.B. Dean, J.D. Bristow, Tenascin-C deficiency attenuates TGF-ß-mediated fibrosis following murine lung injury, Am. J. Phys. Lung Cell. Mol. Phys. 299 (2010) L785–L793, https://doi.org/10.1152/ajplung.00385.2009.

[7] D. Zhang, Z. Liu, Q. Liu, H. Lan, J. Peng, X. Liu, W. Liu, Tenascin-C participates pulmonary injury induced by Paraquat through regulating TLR4 and TGF-β signaling pathways, Inflammation 45 (2022) 222–233, https://doi.org/10.1007/s10753-021-01540-w.

[8] T. Takahashi, Y. Asano, Y. Ichimura, T. Toyama, T. Taniguchi, S. Noda, K. Akamata, Y. Tada, M. Sugaya, T. Kadono, S. Sato, Amelioration of tissue fibrosis by toll-like receptor 4 knockout in murine models of systemic sclerosis, Arthritis Rheum. 67 (2015) 254–265, https://doi.org/10.1002/art.38901.

[9] S. Bhattacharyya, K.S. Midwood, J. Varga, Tenascin-C in fibrosis in multiple organs: translational implications, Semin. Cell Dev. Biol. 128 (2022) 130–136, https://doi.org/10.1016/j.semcdb.2022.03.019.

[10] S. Bhattacharyya, K.S. Midwood, H. Yin, J. Varga, Toll-like Receptor-4 signaling drives persistent fibroblast activation and prevents fibrosis resolution in scleroderma, Adv Wound Care (New Rochelle). 6 (2017) 356–369, https://doi.org/10.1089/wound.2017.0732.

[11] S.P. Giblin, K.S. Midwood, Tenascin-C: form versus function, Cell Adhes. Migr. 9 (2015) 48–82, https://doi.org/10.4161/19336918.2014.987587.

[12] K.S. Midwood, S. Sacre, A.M. Piccinini, J. Inglis, A. Trebaul, E. Chan, S. Drexler, N. Sofat, M. Kashiwagi, G. Orend, F. Brennan, B. Foxwell, Tenascin-C is an endogenous activator of toll-like receptor 4 that is essential for maintaining inflammation in arthritic joint disease, Nat. Med. 15 (2009) 774–780, https://doi.org/10.1038/nm.1987.

[13] A.M. Piccinini, K.S. Midwood, Endogenous control of immunity against infection: tenascin-C regulates TLR4-mediated inflammation via microRNA-155, Cell Rep. 2 (2012) 914–926, https://doi.org/10.1016/j.celrep.2012.09.005.

[14] A.M. Piccinini, L. Zuliani-Alvarez, J.M. Lim, K.S. Midwood, Distinct microenvironmental cues stimulate divergent TLR4-mediated signaling pathways in macrophages, Sci. Signal. 9 (2016) ra86, https://doi.org/10.1126/scisignal.aaf3596.

[15] S.M. Opal, P.F. Laterre, B. Francois, S.P. LaRosa, D.C. Angus, J.P. Mira, X. Wittebole, T. Dugernier, D. Perrotin, M. Tidswell, L. Jauregui, K. Krell, J. Pachl, T. Takahashi, C. Peckelsen, E. Cordasco, C.S. Chang, S. Oeyen, N. Aikawa, T. Maruyama, R. Schein, A.C. Kalil, M. Van Nuffelen, M. Lynn, D.P. Rossignol, J. Gogate, M.B. Roberts, J.L. Wheeler, J.L. Vincent, ACCESS Study Group. Effect of eritoran, an antagonist of MD2-TLR4, on mortality in patients with severe sepsis: the ACCESS randomized trial, JAMA 309 (2013) 1154–1162, https://doi.org/10.1001/jama.2013.2194.

[16] C. Tiede, A.A. Tang, S.E. Deacon, U. Mandal, J.E. Nettleship, R.L. Owen, S. E. George, D.J. Harrison, R.J. Owens, D.C. Tomlinson, M.J. McPherson, Adhiron: a stable and versatile peptide display scaffold for molecular recognition applications, Protein Eng. Des. Sel. 27 (2014) 145–155, https://doi.org/10.1093/protein/gzu007.

[17] N. Pechlivani, B. Alsayejh, M. Almutairi, K. Simmons, T. Gaule, F. Phoenix, N. Kietsiriroje, S. Ponnambalam, C. Duval, R.A.S. Ariëns, C. Tiede, D.C. Tomlinson, R.A. Ajjan, Use of Affimer technology for inhibition of α2-antiplasmin and enhancement of fibrinolysis, Blood Adv. 9 (2025) 89–100, https://doi.org/10.1182/bloodadvances.2024014235.

[18] A.A.S. Tang, A. Macdonald, M.J. McPherson, D.C. Tomlinson, Targeting Grb2 SH3 domains with Affimer proteins provides novel insights into Ras Signalling modulation, Biomolecules 14 (2024) 1040, https://doi.org/10.3390/biom14081040.

[19] R.G. Xu, C. Tiede, A.N. Calabrese, L.T. Cheah, T.L. Adams, J.S. Gauer, M.S. Hindle, B.A. Webb, D.M. Yates, A. Slater, C. Duval, K.M. Naseem, A.B. Herr, D. C. Tomlinson, S.P. Watson, R.A.S. Ariëns, Affimer reagents as tool molecules to modulate platelet GPVI-ligand interactions and specifically bind GPVI dimer, Blood Adv. 8 (2024) 3917–3928, https://doi.org/10.1182/bloodadvances.2024012689.

[20] B.W.R. Roper, C. Tiede, I. Abdul-Zani, G.A. Cuthbert, D. Jade, A. Al-Aufi, W. R. Critchley, Q. Saikia, S. Homer-Vanniasinkam, T. Sawamura, M.J. McPherson, M. A. Harrison, D.C. Tomlinson, S. Ponnambalam, "Affimer" synthetic protein scaffolds block oxidized LDL binding to the LOX-1 scavenger receptor and inhibit ERK1/2 activation, J. Biol. Chem. 299 (2023) 105325, https://doi.org/10.1016/j.jbc.2023.105325.

[21] H.L. Martin, A.L. Turner, J. Higgins, A.A. Tang, C. Tiede, T. Taylor, S. Siripanthong, T.L. Adams, I.W. Manfield, S.M. Bell, E.E. Morrison, J. Bond, C.H. Trinh, C. D. Hurst, M.A. Knowles, R.W. Bayliss, D.C. Tomlinson, Affimer-mediated locking of p21-activated kinase 5 in an intermediate activation state results in kinase inhibition, Cell Rep. 31 (2023) 113184, https://doi.org/10.1016/j.celrep.2023.113184.

[22] K.Z. Haza, H.L. Martin, A. Rao, A.L. Turner, S.E. Saunders, B. Petersen, C. Tiede, K. Tipping, A.A. Tang, M. Ajayi, T. Taylor, M. Harvey, K.M. Fishwick, T.L. Adams, T.G. Gaule, C.H. Trinh, M. Johnson, A.L. Breeze, T.A. Edwards, M.J. McPherson, D. C. Tomlinson, RAS-inhibiting biologics identify and probe druggable pockets including an SII-α3 allosteric site, Nat. Commun. 12 (2021) 4045, https://doi.org/10.1038/s41467-021-24316-0.

[23] R.J. King, K. Schuett, C. Tiede, V. Jankowski, V. John, A. Trehan, K. Simmons, S. Ponnambalam, R.F. Storey, C.W.G. Fishwick, M.J. McPherson, D.C. Tomlinson, R.A. Ajjan, Fibrinogen interaction with complement C3: a potential therapeutic target to reduce thrombosis risk, Haematologica 10 (2021) 1616–1623, https://doi.org/10.3324/haematol.2019.239558.

[24] K.J. Kearney, N. Pechlivani, R. King, C. Tiede, F. Phoenix, R. Cheah, F.L. Macrae, K. J. Simmons, I.W. Manfield, K.A. Smith, B.E.J. Spurgeon, K.M. Naseem, R.A. S. Ariens, M.J. McPherson, D.C. Tomlinson, R.A. Ajjan, Affimer proteins as a tool to modulate fibrinolysis, stabilize the blood clot, and reduce bleeding complications, Blood 133 (2019) 1233–1244, https://doi.org/10.1182/blood-2018-06-856195.

[25] J.I. Robinson, E.W. Baxter, R.L. Owen, M. Thomsen, D.C. Tomlinson, M. P. Waterhouse, S.J. Win, J.E. Nettleship, C. Tiede, R.J. Foster, R.J. Owens, C.W. G. Fishwick, S.A. Harris, A. Goldman, M.J. McPherson, A.W. Morgan, Affimer proteins inhibit immune complex binding to FcγRIIIa with high specificity through competitive and allosteric modes of action, Proc. Natl. Acad. Sci. USA 115 (2018) E72–E81, https://doi.org/10.1073/pnas.1707856115.

[26] M.A. Michel, K.N. Swatek, M.K. Hospenthal, D. Komander, Ubiquitin linkage-specific Affimers reveal insights into K6-linked ubiquitin signaling, Mol. Cell 68 (2017) 233–246.e5, https://doi.org/10.1016/j.molcel.2017.08.020.

[27] A. Lawson, Antibody-enabled small-molecule drug discovery, Nat. Rev. Drug Discov. 11 (2012) 519–525, https://doi.org/10.1038/nrd3756.

[28] C. Tiede, R. Bedford, S.J. Heseltine, G. Smith, I. Wijetunga, R. Ross, D. AlQallaf, A. P. Roberts, A. Balls, A. Curd, R.E. Hughes, H. Martin, S.R. Needham, L.C. Zanetti-Domingues, Y. Sadigh, T.P. Peacock, A.A. Tang, N. Gibson, H. Kyle, G.W. Platt, N. Ingram, T. Taylor, L.P. Coletta, I. Manfield, M. Knowles, S. Bell, F. Esteves, A. Maqbool, R.K. Prasad, M. Drinkhill, R.S. Bon, V. Patel, S.A. Goodchild, M. Martin-Fernandez, R.J. Owens, J.E. Nettleship, M.E. Webb, M. Harrison, J. D. Lippiat, S. Ponnambalam, M. Peckham, A. Smith, P.K. Ferrigno, M. Johnson, M. J. McPherson, D.C. Tomlinson, Affimer proteins are versatile and renewable affinity reagents, Elife 6 (2017) e24903, https://doi.org/10.7554/eLife.24903.

[29] S.H. Shamsuddin, D.G. Jayne, D.C. Tomlinson, M.J. McPherson, P.A. Millner, Selection and characterisation of Affimers specific for CEA recognition, Sci. Rep. 11 (2021) 744, https://doi.org/10.1038/s41598-020-80354-6.

[30] L. Zuliani-Alvarez, A.M. Marzeda, C. Deligne, A. Schwenzer, F.E. McCann, B. D. Marsden, A.M. Piccinini, K.S. Midwood, Mapping tenascin-C interaction with toll-like receptor 4 reveals a new subset of endogenous inflammatory triggers, Nat. Commun. 8 (2017) 1595, https://doi.org/10.1038/s41467-017-01718-7.

[31] P.C. Hawkins, A.G. Skillman, A. Nicholls, Comparison of shape-matching and docking as virtual screening tools, J. Med. Chem. 11 (2007) 74–82, https://doi.org/10.1021/jm0603365.

[32] G.M. Sastry, M. Adzhigirey, T. Day, R. Annabhimoju, W. Sherman, Protein and ligand preparation: parameters, protocols, and influence on virtual screening enrichments, J. Comput. Aid. Mol. Des. 27 (2013) 221–234, https://doi.org/10.1007/s10822-013-9644-8.

[33] F. van den Hoogen, D. Khanna, J. Fransen, S.R. Johnson, M. Baron, A. Tyndall, M. Matucci-Cerinic, R.P. Naden, T.A. Medsger Jr., P.E. Carreira, G. Riemekasten, P. J. Clements, C.P. Denton, O. Distler, Y. Allanore, D.E. Furst, A. Gabrielli, M. D. Mayes, J.M. van Laar, J.R. Seibold, L. Czirjak, V.D. Steen, M. Inanc, O. Kowal-Bielecka, U. Müller-Ladner, G. Valentini, D.J. Veale, M.C. Vonk, U.A. Walker, L. Chung, D.H. Collier, M. Ellen Csuka, B.J. Fessler, S. Guiducci, A. Herrick, V. M. Hsu, S. Jimenez, B. Kahaleh, P.A. Merkel, S. Sierakowski, R.M. Silver, R. W. Simms, J. Varga, J.E. Pope, Classification criteria for systemic sclerosis: An ACR-EULAR Collaborative Initiative, Ann. Rheum. Dis. 72 (2013) (2013) 1747–1755. DOI: 10.1136/annrheumdis-2013-204424. DOI: 10.1136/annrheumdis-2013-204424.

[34] L.S. Lonzetti, F. Joyal, J.P. Raynauld, A. Roussin, J.R. Goulet, E. Rich, D. Choquette, Y. Raymond, J.L. Senécal, Updating the American College of Rheumatology preliminary classification criteria for systemic sclerosis: addition of severe nailfold capillaroscopy abnormalities markedly increases the sensitivity for limited scleroderma, Arthritis Rheum. 44 (2001) 735–736, https://doi.org/10.1002/1529-0131(200103)44:3<735::AID-ANR125>3.0.CO;2-F.

[35] M. Matucci-Cerinic, Y. Allanore, L. Czirják, A. Tyndall, U. Müller-Ladner, C. Denton, G. Valentini, O. Distler, K. Fligelstone, A. Tyrrel-Kennedy, D. Farge, O. Kowal-Bielecka, F. van den Hoogen, M. Cutolo, P.D. Sampaio-Barros, P. Nash, K. Takehara, D.E. Furst, The challenge of early systemic sclerosis for the EULAR scleroderma trial and research group (EUSTAR) community. It is time to cut the Gordian knot and develop a prevention or rescue strategy, Ann. Rheum. Dis. 68 (2009) 1377–1380, https://doi.org/10.1136/ard.2008.106302.

[36] J. Avouac, J. Fransen, U.A. Walker, V. Riccieri, V. Smith, C. Muller, I. Miniati, I. H. Tarner, S. Bellando Randone, M. Cutolo, Y. Allanore, O. Distler, G. Valentini, L. Czirjak, U. Müller-Ladner, D.E. Furst, A. Tyndall, M. Matucci-Cerinic, EUSTAR Group, Preliminary criteria for the very early diagnosis of systemic sclerosis: results of a Delphi consensus study from EULAR scleroderma trials and research group, Ann. Rheum. Dis. 70 (2011) 476–481, https://doi.org/10.1136/ard.2010.136929.

[37] E.C. LeRoy, C. Black, R. Fleischmajer, S. Jablonska, T. Krieg, T.A. Medsger Jr., N. Rowell, F. Wollheim, Scleroderma (systemic sclerosis): classification, subsets and pathogenesis, J. Rheumatol. 15 (1988) 202–205 (PMID: 3361530).
[38] J. Gillespie, R.L. Ross, C. Corinaldesi, F. Esteves, E. Derrett-Smith, M.F. McDermott, G.M. Doody, C.P. Denton, P. Emery, F. Del Galdo, Transforming growth factor β activation primes canonical Wnt signaling through Down-regulation of Axin-2, Arthritis Rheum. 70 (2018) 932–942, https://doi.org/10.1002/art.40437.
[39] R.L. Ross, B. Caballero-Ruiz, E.L. Clarke, V. Kakkar, C.W. Wasson, P. Mulipa, E. De Lorenzis, W. Merchant, S. Di Donato, A. Rindone, A.L. Herrick, C.P. Denton, N. A. Riobo-Del Galdo, F. Del Galdo, Biological hallmarks of systemic sclerosis are present in the skin and serum of patients with very early diagnosis of systemic sclerosis (VEDOSS), Rheumatology keae698 (2024), https://doi.org/10.1093/rheumatology/keae698.
[40] C. Zhang, X. Meng, Z. Zhu, J. Liu, A. Deng, Connective tissue growth factor regulates the key events in tubular epithelial to myofibroblast transition in vitro, Cell Biol. Int. 28 (2004) 863–873, https://doi.org/10.1016/j.cellbi.2004.09.003.
[41] T. Shimo, M. Kanyama, C. Wu, H. Sugito, P.C. Billings, W.R. Abrams, J. Rosenbloom, M. Iwamoto, M. Pacifici, E. Koyama, Expression and roles of connective tissue growth factor in Meckel's cartilage development, Dev. Dyn. 231 (2004) 136–147, https://doi.org/10.1002/dvdy.20109.
[42] C. Capparelli, D. Whitaker-Menezes, C. Guido, R. Balliet, T.G. Pestell, A. Howell, S. Sneddon, R.G. Pestell, U. Martinez-Outschoorn, M.P. Lisanti, F. Sotgia, CTGF drives autophagy, glycolysis and senescence in cancer-associated fibroblasts via HIF1 activation, metabolically promoting tumor growth, Cell Cycle 11 (2012) 2272–2284, https://doi.org/10.4161/cc.20717.
[43] S.J. Heseltine, G.J. Billenness, H.L. Martin, C. Tiede, A.A.S. Tang, E. Foy, G. Reddy, N. Gibson, M. Johnson, M.E. Webb, M.J. McPherson, D.C. Tomlinson, Generating and validating renewable affimer protein binding reagents targeting SH2 domains, Sci. Rep. 14 (2024) 28322, https://doi.org/10.1038/s41598-024-79357-4.
[44] A.A. Tang, C. Tiede, D.J. Hughes, M.J. McPherson, D.C. Tomlinson, Isolation of isoform-specific binding proteins (Affimers) by phage display using negative selection, Sci. Signal. 10 (2017) eaan0868, https://doi.org/10.1126/scisignal.aan0868.
[45] L.J. Randall, S. Bajan, T.D. Tran, R.J. Harvey, F.D. Russell, Propolis compound inhibits profibrotic TGF-β1/SMAD signalling in human fibroblasts, Sci. Rep. 15 (2025) 27260, https://doi.org/10.1038/s41598-025-07918-2.
[46] T. Higuchi, K. Takagi, A. Tochimoto, Y. Ichimura, T. Norose, Y. Katsumata, I. Masuda, H. Yamanaka, T. Morohoshi, Y. Kawaguchi, Antifibrotic effects of 2-carba cyclic phosphatidic acid (2ccPA) in systemic sclerosis: contribution to the novel treatment, Arthritis Res. Ther. 21 (2019) 103, https://doi.org/10.1186/s13075-019-1881-3.
[47] R.L. Ross, B. Caballero-Ruiz, E.L. Clarke, V. Kakkar, C.W. Wasson, P. Mulipa, E. De Lorenzis, W. Merchant, S. Di Donato, A. Rindone, A.L. Herrick, C.P. Denton, N. A. Riobo-Del Galdo, F. Del Galdo, Biological hallmarks of systemic sclerosis are present in the skin and serum of patients with very early diagnosis of systemic sclerosis (VEDOSS), Rheumatology 64 (2025) 3606, https://doi.org/10.1093/rheumatology/keae698.
[48] Y.E. Choi, M.J. Song, M. Hara, K. Imanaka-Yoshida, D.H. Lee, J.H. Chung, S.T. Lee, Effects of tenascin C on the integrity of extracellular matrix and skin aging, Int. J. Mol. Sci. 21 (2020) 8693, https://doi.org/10.3390/ijms21228693.
[49] Y. Zhou, X.Y. Ma, J.Y. Han, M. Yang, C. Lv, Y. Shao, Y.L. Wang, J.Y. Kang, Q. Y. Wang, Metformin regulates inflammation and fibrosis in diabetic kidney disease through TNC/TLR4/NF-κB/miR-155-5p inflammatory loop, World J. Diabetes 12 (2021) 19–46, https://doi.org/10.4239/wjd.v12.i1.19.
[50] Z. Yang, Z. Sun, H. Liu, Y. Ren, D. Shao, W. Zhang, J. Lin, J. Wolfram, F. Wang, S. Nie, Connective tissue growth factor stimulates the proliferation, migration and differentiation of lung fibroblasts during paraquat-induced pulmonary fibrosis, Mol. Med. Rep. 12 (2015) 1091–1097, https://doi.org/10.3892/mmr.2015.3537.
[51] K. Raza, A. Schwenzer, M. Juarez, P. Venables, A. Filer, C.D. Buckley, K. S. Midwood, Detection of antibodies to citrullinated tenascin-C in patients with early synovitis is associated with the development of rheumatoid arthritis, RMD Open 2 (2016) e000318, https://doi.org/10.1136/rmdopen-2016-000318.
[52] M.E. Lacouture, J.C. Morris, D.P. Lawrence, A.R. Tan, T.E. Olencki, G.I. Shapiro, B. J. Dezube, J.A. Berzofsky, F.J. Hsu, J. Guitart, Cutaneous keratoacanthomas/squamous cell carcinomas associated with neutralization of transforming growth factor beta by the monoclonal antibody fresolimumab (GC1008), Cancer Immunol. Immunother. 64 (2015) 437–446, https://doi.org/10.1007/s00262-015-1653-0.
[53] T. Nishioka, M. Suzuki, K. Onishi, N. Takakura, H. Inada, T. Yoshida, M. Hiroe, K. Imanaka-Yoshida, Eplerenone attenuates myocardial fibrosis in the angiotensin II-induced hypertensive mouse: involvement of tenascin-C induced by aldosterone-mediated inflammation, J. Cardiovasc. Pharmacol. 49 (2007) 261–268, https://doi.org/10.1097/FJC.0b013e318033dfd4.
[54] S. Estany, V. Vicens-Zygmunt, R. Llatjós, A. Montes, R. Penín, I. Escobar, A. Xaubet, S. Santos, F. Manresa, J. Dorca, M. Molina-Molina, Lung fibrotic tenascin-C upregulation is associated with other extracellular matrix proteins and induced by TGFβ1, BMC Pulm. Med. 14 (2014) 120, https://doi.org/10.1186/1471-2466-14-120.
[55] M.S. Islam, M. Kusakabe, K. Horiguchi, S. Iino, T. Nakamura, K. Iwanaga, H. Hashimoto, S. Matsumoto, T. Murata, M. Hori, H. Ozaki, PDGF and TGF-β promote tenascin-C expression in subepithelial myofibroblasts and contribute to intestinal mucosal protection in mice, Br. J. Pharmacol. 171 (2014) 375–388, https://doi.org/10.1111/bph.12452.
[56] S. Bhattacharyya, K. Kelley, D.S. Melichian, Z. Tamaki, F. Fang, Y. Su, G. Feng, R. M. Pope, G.R. Budinger, G.M. Mutlu, R. Lafyatis, T. Radstake, C. Feghali-Bostwick, J. Varga, Toll-like receptor 4 signaling augments transforming growth factor-β responses: a novel mechanism for maintaining and amplifying fibrosis in scleroderma, Am. J. Pathol. 182 (2013) 192–205, https://doi.org/10.1016/j.ajpath.2012.09.007.
[57] W. Wang, S. Bale, B. Yalavarthi, P. Verma, P.S. Tsou, K.M. Calderone, D. Bhattacharyya, G.J. Fisher, J. Varga, S. Bhattacharyya, Deficiency of inhibitory TLR4 homolog RP105 exacerbates fibrosis, JCI Insight 7 (2022) e160684, https://doi.org/10.1172/jci.insight.160684.